Visibility of Halftone Dot Textures

RISTO NÄSÄNEN

Abstract—**A calculational method for estimating the visibility of halftone dot textures is presented. The visibility estimations can be utilized in dither signal designing. The method is based on the properties of human visual contrast sensitivity. The accuracy of the calculated visibility estimations was tested experimentally with dot textures produced by four different kinds of dither signals. The visibility predictions agreed very well with the results of psychophysical measurements.**

I. Introduction

One basic factor affecting the perceptual image quality of halftone images is the visibility of halftone dot textures. The poorer that the visual appearance of continuous tone is, the more visible the dot textures are. Visible dot textures are experienced as disturbing because they contain visual information that is irrelevant for the viewer. In addition, the visibility of dot textures are usually inversely related to perceived image sharpness because visible dot textures are coarse-grained and their ability to convey detailed image information is poor. Qualitatively these effects can be seen in the portrait in Fig. 1, where the dot texture visibility is varied either by reducing picture element size or by using a less coarse-grained dot texture structure.

The present correspondence proposes a method for the quantitative estimation of the visibility of periodic halftone dot textures generated by the ordered dither technique. The method can be used for designing dither signals. Dither signals determine the structural properties of halftone dot textures. The estimated visibility is expressed as the visual resolution frequency that is the highest fundamental spatial frequency at which a periodic dot texture is just visible. Predictions based on the proposed method are compared with psychophysical results on four different kinds of dither signals.

II. Method for Estimating the Visibility of Halftone Dot Textures

Halftone images are used in graphic arts and in some computer displays to generate continuous-tone images by means of two luminance levels only (usually black and white). The local spatial average luminance of dark and bright areas of the halftone image varies approximately according to the luminance variations of the original continuous-tone image. The visual appearance of continuous tone is based on the low-pass filtering performed by the visual system. High-frequency variation of dark and bright areas is strongly attenuated in the visual system, but local spatial averages, i.e., the actual image information, remain visible.

Ordered dither is a commonly used method for generating halftone images. The halftone conversion is achieved by thresholding each image sample by a dither signal. In the halftone image a display site $(g_{n,m})$ will be in bright state if the corresponding image sample value $(s_{n,m})$ exceeds the threshold $(t_{n,m})$

$$g_{n,m} = \begin{cases} 1, & \text{if } s_{n,m} \geq t_{n,m} \\ 0, & \text{otherwise.} \end{cases}$$

The dither signal is a matrix of uniformly distributed thresholds that is repeated in two dimensions over the image. For constant luminances, halftone dot textures are periodic. The set of dot textures for all gray levels is called [1] the dot profile.

One halftone dot texture period $g(x, y)$ can be described as

$$g(x,y) = \sum_{n=0}^{N-1} \sum_{m=0}^{N-1} g_{n,m} \operatorname{rect}((x - nR)/R, (y - mR)/R)$$

where $g_{n,m}$ is an $N \times N$ array of zeros and unities giving the intensity value for each display site in the dot texture period. The *rect*-function describes the rectangular luminance profile of one $R \times R$ display site located in (nR, mR). Fig. 2 shows an example of a 5×5 dot texture period.

Fourier series coefficients for $g(x, y)$ are

$$F(u,v) = \operatorname{sinc}(u/N) \operatorname{sinc}(v/N) \frac{1}{N^2} \sum_{n=0}^{N-1} \cdot \sum_{m=0}^{N-1} g_{n,m} e^{-j2\pi(nu+mv)/N},$$

where $\operatorname{sinc}(x) = \sin(\pi x)/(\pi x)$ (see Appendix). Fourier series coefficients can be changed to correspond to the actual luminances in the display

$$F^L(u,v) = (L_{\max} - L_{\min}) F(u,v), \quad \text{when } u, v \neq 0, \text{ and}$$

$$F^L(0,0) = (L_{\max} - L_{\min}) F(0,0) + L_{\min}$$

where L_{max} and L_{min} are the maximum and minimum luminances (luminances of bright and dark display sites).

Visual contrast sensitivity describes the signal processing properties of the visual system near threshold contrast. For sinusoidal gratings contrast is defined as

$$C = \frac{L_{\max} - L_{\min}}{L_{\max} + L_{\min}} = \frac{A}{L}$$

where L_{max} and L_{min} are the maximum and minimum luminances, respectively, A is the luminance amplitude and L is the average luminance. Contrast sensitivity is the reciprocal of contrast threshold. Because there is some uncertainty in contrast detection near the threshold, the contrast threshold may be defined as the contrast at which the stimulus is detected by a given probability smaller than unity. The contrast sensitivity function describes contrast sensitivity for sinusoidal gratings as a function of spatial frequency. spatial frequency is usually expressed in cycles per degree of visual angle (c/deg).

The descending part of the visual contrast sensitivity function CS at spatial frequencies f higher than about 2 c/deg can be described by an exponential function [2]

$$CS = Se^{-\alpha f} \tag{1}$$

where S and α are parameters whose values depend on the average luminance. The slope of the exponential contrast sensitivity function decreases when average luminance is increased. This is shown in Fig. 3. This means that contrast sensitivity increases more slowly for low than high spatial frequencies as a function of average luminance. Thus parameters S and α in (1) are functions of average luminance L. The data of Fig. 3 can be described by the following equation

$$CS = S(L) e^{-\alpha(L) f} \tag{2}$$

where

$$S(L) = aL^b, \text{ and} \tag{3}$$

$$\alpha(L) = \frac{k}{c \ln(L) + d} \tag{4}$$

and a, b, c, d, and k are constants (see Fig. 3).

Visual sensitivity is usually better for horizontal and vertical line orientations than for oblique orientations when possible eye

Manuscript received November 22, 1983; revised June 1984.

The author is with the Laboratory of Graphic Arts Technology, Helsinki University of Technology, and the Division of General Psychology, University of Helsinki, Ritarikatu 5, SF00170 Helsinki 17, Finland.

0018-9472/84/1100-0920$01.00 ©1984 IEEE

(a) (b) (c)

Fig. 1. Demonstration of the effects of halftone dot texture visibility. (a) Disturbing effects of a clearly visible dot texture. (b) Effects may be reduced by reducing the pixel size and consequently increasing the number of pixels. (c) Effects may be reduced to some extent by using a less coarse-grained dot texture structure. The number of image samples is the same in each image. In (a) and (c) the number of output pixels is the same as the number of image samples. Image (b) is processed at twice the sampled resolution thus having a fourfold number of output pixels. The halftone conversion was performed by the ordered dither technique using the 8 × 8 diamond dot profile in (a) and (b) and the 8 × 8 grating dot profile in (c).

1	1	0	1	1
1	0	0	0	1
0	0	0	0	0
1	0	0	0	1
1	1	0	1	1

Fig. 2. Example of a 5 × 5 halftone dot period. Dark elements have a value equal to zero, and bright elements have a value equal to unity.

astigmatism is corrected. However, in large populations the differences between contrast sensitivities for different orientations are very small [2]. Thus the orientation effect probably does not possess any considerable practical significance, and the exponential contrast sensitivity function can be assumed to be circularly symmetric in the two-dimensional frequency domain.

Since contrast sensitivity CS is the reciprocal of threshold contrast C_T contrast sensitivity for high spatial frequencies from (2) can be written as

$$\frac{1}{C_T} = S(L)\, e^{-\alpha(L)f}. \tag{5}$$

Visual resolution frequency for a sinusoidal grating having a constant contrast C can be calculated from (5) because contrast threshold is the contrast C of the grating, and (5) may be written as

$$1 = CS(L)\, e^{-\alpha(L)f}. \tag{6}$$

Solving frequency f from (6) gives the visual resolution frequency for any given constant contrast C. The right side of (6) is called the visual contrast response.

If there are many harmonic frequency components, as in periodic halftone dot textures, the contrast response has to be combined somehow from the components. Contrast sensitivity for complex luminance waveforms is better described by multiple-channel models than by single-channel models [4]–[8]. A multiple-channel model assumes that different parts of the image spectrum are simultaneously processed by different mechanisms in the visual system. Each of these mechanisms, called channels, transmits only a relatively narrow band of frequencies. The vector–magnitude principle proposed by Quick [7] for integration of channel outputs is found to well predict the contrast sensitivities for complex cratings [8]. According to Quick's principle, the contrast response (CR) of the whole system is combined from the channel outputs as the vector–magnitude

$$CR = \left[\sum_i |z_i|^p\right]^{1/p}$$

where z_i is the output of channel i, and p is a constant approximately in the range of 3 to 4 [8]. An intermediate value of 3.5 is used here.

It is assumed here, for simplicity, that each channel transmits only one harmonic frequency component of the periodic image signal without having any effect on its amplitude. That is, the contrast response is directly combined from the exponentially filtered frequency components according to the vector–magnitude principle

$$CR = \left[\sum_i |C_i S(L)\, e^{-\alpha(L)f_i}|^p\right]^{1/p}$$

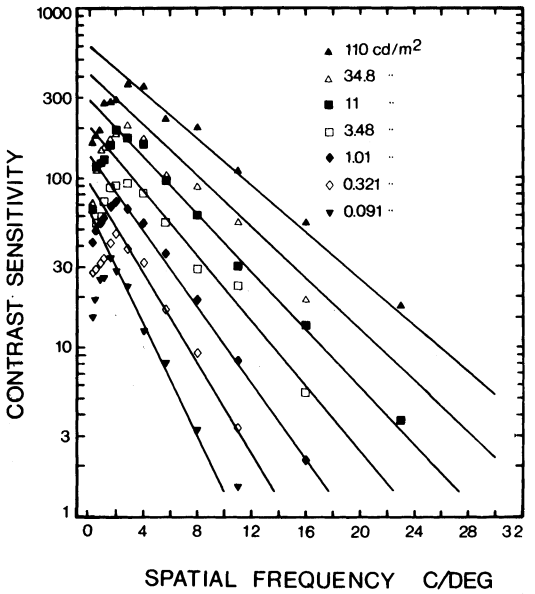

Fig. 3. Visual contrast sensitivity functions for various average luminances. Vertical gratings presented for 1.0 s at each detection trial and subtending 2.5° in diameter were viewed monocularly at a distance of 256 cm in the contrast threshold determinations (from unpublished data of the author and V. Virsu). Contrast sensitivity axis is logarithmic, and frequency axis is linear to show the exponentiality of the descending part of contrast sensitivity functions at high spatial frequencies. Symbols refer to experimental findings, and solid lines refer to calculated values based on (2)–(4) with constants $a = 131.6$, $b = 0.3188$, $c = 0.525$, $d = 3.91$, and $k = 1$.

where C_i is the contrast of ith harmonic, and f is the fundamental spatial frequency of the periodic image signal. If the contrast response is greater than unity the image signal is visible. If the contrast response is equal to unity, the image signal is just at the contrast threshold.

According to the principles just given, the visual resolution frequency for periodic two-dimensional luminance waveforms, such as periodic halftone dot textures, can be calculated by solving the fundamental frequency f from the following equation

$$\left[\sum_{u=\pm 1}^{\pm\infty} \sum_{v=\pm 1}^{\pm\infty} |S(L)\, e^{-\alpha(L) f_r} |F(u,v)|/L|^p \right]^{1/p} = 1 \qquad (7)$$

where the left side is the visual contrast response,

$$f_r = f[u^2 + v^2]^{1/2}$$

and L is the average luminance or the zero frequency component. $|F(u,v)|$ is the amplitude spectrum of the luminance waveform

$$|F(u,v)| = \left[R^2(u,v) + I^2(u,v) \right]^{1/2}$$

where $R(u,v)$ and $I(u,v)$ are the real and imaginary components of the complex Fourier series corrected to correspond to the luminances of the display.

III. Experimental Methods

Visual resolution frequencies were measured for the following four kinds of halftone dot profiles: 1) an 8 × 8 diamond dot profile that contains in each dot cycle one approximately diamond-shaped dot, the size of which varies according to the gray level; 2) an 8 × 8 line dot profile that consists of lines whose width varies according to the gray level, 3) a 5 × 5 dot profile proposed by Bryngdahl [9]; and 4) a 4 × 4 grating dot profile that satisfies the optimality conditions of Bayer [10]. In dot profiles 3) and 4) there is not a single dot or line in one dot texture period, but many small dots scattered more or less uniformly within the area of one period.

TABLE I
Dither Matrices for 8 × 8 Diamond Dot Profile, 8 × 8 Line Dot Profile, Bryngdahl's 5 × 5 Dot Profile and 4 × 4 Grating Dot Profile

61	53	41	33	37	52	60	64
57	45	25	13	17	32	48	56
49	29	21	5	9	24	28	44
39	19	11	1	3	8	16	36
35	15	7	4	2	12	20	40
43	27	23	10	6	22	30	50
55	47	31	18	14	26	46	58
63	59	51	38	34	42	54	62

(a)

1	2	3	4	5	6	7	8
1	2	3	4	5	6	7	8
1	2	3	4	5	6	7	8
1	2	3	4	5	6	7	8
1	2	3	4	5	6	7	8
1	2	3	4	5	6	7	8
1	2	3	4	5	6	7	8
1	2	3	4	5	6	7	8

(b)

9	1	12	10	7
3	23	21	14	24
13	17	4	6	18
11	19	8	2	16
5	25	15	20	22

(c)

1	9	3	11
13	5	15	7
4	12	2	10
16	8	14	6

(d)

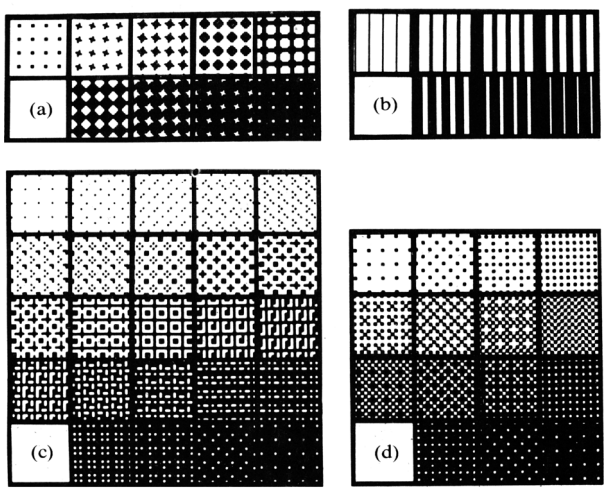

Fig. 4. Examples of dot profiles used in the visual resolution experiment. (a) 8 × 8 diamond dot profiles. (b) 8 × 8 line dot profile. (c) Bryngdahl's 5 × 5 dot profile. (d) 4 × 4 grating dot profile.

The dither matrices for these dot profiles are given in Table I, and examples of the dot textures are shown in Fig. 4. The dither thresholds $t_{n,m}$ are based on the dither matrix values $d_{n,m}$ in the following way when the image signal is normalized between zero and unity:

$$t_{n,m} = (d_{n,m} - 1/2)/(N \times N)$$

where $N \times N$ is the size of the dither matrix.

The dot textures were produced on film by a computer controlled film plotter (Optronix P1500). The dot textures were displayed by means of a projector, one gray level at a time. The display aperture was rectangular and was surrounded by a cardboard, the luminance of which was 50 cd/m^2. The luminances of the dark and bright parts of the dot textures were 70 and 500 cd/m^2, respectively.

A method of adjustment was used as a psychophysical method because of it's simplicity. More sophisticated methods, such as the forced-choice methods, would have been unnecessarily laborous here because the number of different measurements was large.

The visual resolution frequencies for the dot profiles at different gray levels were measured by changing the viewing distance.

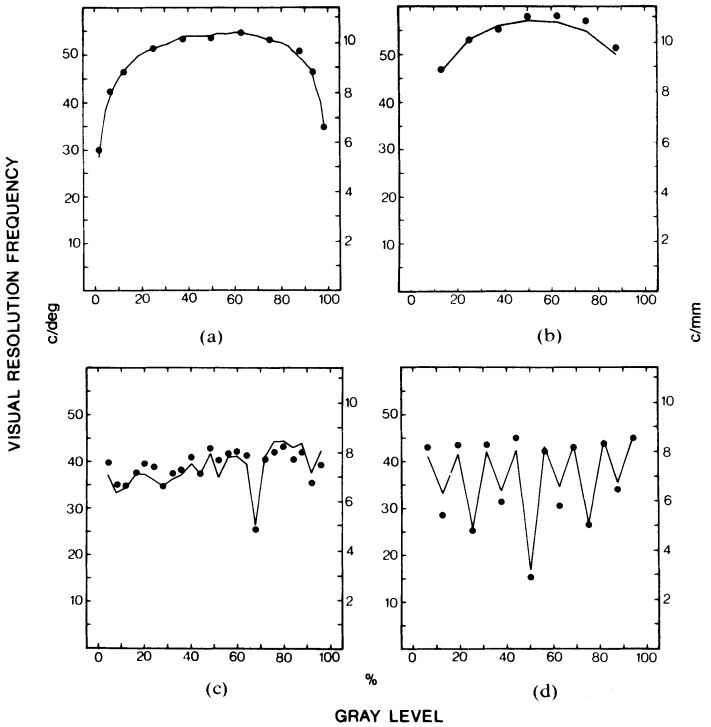

Fig. 5. Visual resolution frequencies as a function of gray level for the following. (a) 8 × 8 grating dot profile. (b) 8 × 8 line dot profile. (c) Bryngdahl's 5 × 5 dot profile. (d) 4 × 4 grating dot profile. Symbols refer to experimental results, and solid lines refer to theoretical calculations. In theoretical calculations the values of the constants of (2)–(4) were the same as for the contrast sensitivity data of Fig. 2, except value of constant $k = 0.85$ was estimated from the experimental data for diamond dot profile. Value of exponent $p = 3.5$ in (7) was chosen on the bases of [8]. Visual resolution frequencies are expressed in cycles/deg of visual angle on left and for a viewing distance of 30 cm in cycles/mm on right. Gray levels are expressed in percentage of dark display sites.

The observer first moved slowly backwards until he could not resolve any luminance variations in the dot texture. This viewing distance was measured. After this he moved slightly farther, and then he moved slowly forwards until he just could see the texture. The viewing distance was measured again. This procedure was repeated for each gray level of each dot profile from bright tones to dark tones. The whole experiment was then repeated in a reverse order Thus there were four measurements for each gray level of each dot profile. The total number of measurements was 228.

The measured viewing distances were converted into visual resolution frequencies by using the following formula:

$$f_{c/\text{deg}} = \frac{\pi s f_d}{180}$$

where $f_{c/\text{deg}}$ is frequency expressed in cycles per degree of visual angle, f_d is frequency in the display (cycles/cm), and s is viewing distance (cm).

The observer in the main experiment was the author. Two other persons served as observers in control experiments.

IV. Results

The visual resolution frequencies as a function of gray level for each dot profile are shown in Fig. 5. Gray levels are expressed in percentage of the portion of dark elements in one dot pattern cycle. For example, if the gray level value is zero percent, then all display sites are in bright state, and if the gray-level value is 100 percent then, all display sites are in dark state. Standard deviations of the measurements for each gray level expressed in percentage of the mean varied between one and ten percent. Control experiments with two other observers gave similar results, except that the average level of the resolution values was slightly lower.

The solid lines in Fig. 5 show theoretical resolution values. They were calculated by solving (7) numerically in the following way: contrast responses were calculated for an increasing series of fundamental dot texture frequencies f so that the ratio of successive frequencies was $\sqrt{2}$. The frequency value that produces a contrast response equal to unity, the resolution frequency, was interpolated by using logarithms of contrast responses for two successive frequencies one of which was the first frequency that produced a contrast response below unity, and the other was the preceeding frequency. The values of parameters in (2)–(4) were the same as for the contrast sensitivity data of Fig. 3 except that the value of parameter k (0.85) was estimated from the experimental data for the diamond dot profile.

V. Conclusion

The theoretical resolution curves in Fig. 5 agree very well with the experimental resolution values for the four structurally different dot profiles, indicating that the method for estimating visual resolution frequencies is accurate enough for practical purposes.

In practice the visibility of dot textures may be reduced in two ways. The pixel size may be reduced, which leads to higher fundamental texture frequency and decreases texture visibility (as in Fig. 1 (a) and (b)). As a result, the number of pixels increase, and consequently the amount of data processing increases, too. In addition, this approach is not always possible because the pixel size of an output device may be limited. Another possibility is to design less coarse-grained dot profiles, the visibilities of which are lower (an example of this approach is in Fig. 1 (c)). This reduces the need for small pixel sizes and extensive data processing. The present method can be used for obtaining rapid quantitative visibility predictions when solving problems of this kind.

We have actually examined only one aspect of visibility here, the resolution limit, but not the effects of visible dot textures whose fundamental frequencies are below the resolution limit of the visual system. The ground for the validity of present ap-

proach is in the fact that in printed images the fundamental dot texture frequencies are usually relatively close to the resolution limit of the visual system. On the other hand, in computer displays dot textures are usually clearly visible because of larger pixel sizes. It is not clear yet whether the present method can be applied to the latter case or not. Instead of calculated resolution frequencies, calculated contrast responses for dot textures with a given fundamental frequency (left side of (7)) might be more appropriate for describing the disturbances caused by visible dot textures.

The perceptual quality of halftone images is based on many factors such as the visibility of dot textures, the perceived image sharpness, and the undesirability of visible dot textures. For the ordered dither technique, the problem is to find dither signals for which these factors are in optimum relation with each other. This optimization involves quantitative measures for the quality factors. This correspondence gives a calculational method for quantitatively evaluating one of these factors, the visibility of halftone dot textures.

Appendix: Fourier Series Coefficients for Periodic Halftone Dot Textures

For a periodic waveform $g(x)$ with period T Fourier series coefficients are

$$F(u) = \frac{1}{T}\int_{-T/2}^{T/2} g(x)\, e^{-j2\pi ux/T}\, dx;$$

$$u = 0, \pm 1, \pm 2, \pm 3 \cdots.$$

One-dimensional halftone dot patterns can be described as

$$g(x) = \sum_{n=0}^{N-1} g_n \,\mathrm{rect}\left((x - nR)/R\right)$$

where g_n is an one dimensional array of zeros and unities with N elements and R is the width of one display site. The width of one period is NR. Fourier series coefficients for $g(x)$ are

$$F(u) = \frac{1}{NR}\int_{-R/2}^{(N-1/2)R} \sum_{n=0}^{N-1} g_n \,\mathrm{rect}\left((x - nR)/R\right) \cdot e^{-j2\pi ux/(NR)}\, dx.$$

After changing the order of integration and summation we have

$$F(u) = \frac{1}{NR}\sum_{n=0}^{N-1} g_n \int_{-R/2}^{(N-1/2)R} \mathrm{rect}\left((x - nR)/R\right) \cdot e^{-j2\pi ux/(NR)}\, dx.$$

The integration gives the Fourier transform of the *rect*-function. The Fourier transform of a not shifted *rect*-function $rect(x/R)$ is $R\,\mathrm{sinc}(u/N)$. When the rect-function is shifted by nR the Fourier transform has to be multiplied by $\exp(-j2\pi nRu/(NR))$ according to the shift theorem. After substitution and reduction we have

$$F(u) = \mathrm{sinc}(u/N)\frac{1}{N}\sum_{n=0}^{N-1} g_n e^{-j2\pi nu/N}.$$

The extension to two dimensions is straightforward.

Acknowledgment

I wish to thank Professor Veijo Virsu for valuable comments on the manuscript. I also wish to thank Professor Hannu Saarelma and Dr. Pekka Kekolahti for their helpful discussions.

References

[1] J. P. Allebach and B. Liu, "Analysis of halftone dot profile and aliasing in the discrete binary representation of images," *J. Opt. Soc. Am.*, vol. 67, pp. 1147–1154, 1977.
[2] V. Virsu, P. Lehtiö, and J. Rovamo, "Contrast sensitivity in normal and pathological vision," *Doc. Ophthal. Proc. Series*, vol. 30, L. Maffei, Ed. The Hague, The Netherlands: Dr. W. Junk Publisher, 1981.
[3] S. Appelle, "Perception and discrimination as a function of stimulus orientation: The "oblique effect" in man animals," *Psychol. Bull.*, vol. 78, pp. 266–278, 1972.
[4] F. W. Campbell and J. G. Robson, "Application of Fourier analysis to the visibility of gratings," *J. Physiol.* vol. 197, pp. 551–566, 1968.
[5] N. Graham and J. Nachmias, "Detection of grating patterns containing two spatial frequencies: A comparison of single-channel and multiple-channels models," *Vision Res.*, vol. 11, pp. 251–259, 1971.
[6] M. B. Sachs, J. Nachmias, and J. G. Robson, "Spatial frequency channels in human vision," *J. Opt. Soc. Am.* vol. 61, pp. 1176–1186, 1971.
[7] R. F. Quick, "A vector-magnitude model of contrast detection," *Kybernetik*, vol. 16, pp. 65–67, 1974.
[8] N. Graham, J. G. Robson, and J. Nachmias, "Grating summation in fovea and periphery," *Vision Res.*, vol. 18, pp. 815–825, 1978.
[9] O. Bryngdahl, "Halftone images: Spatial resolution and tone reproduction," *J. Opt. Soc. Am.*, vol. 68, pp. 416–422, 1978.
[10] B. E. Bayer, "An optimum method for two level rendition of continuous-tone pictures," in *Proc.* IEEE *Int. Conf. on Communication Conference Record*, session 26, pp. 11–15, 1973.

Learning Behavior of Variable-Structure Stochastic Automata in a Three-Person Zero-Sum Game

KENSHIRO OKAMURA, TAIHO KANAOKA, TOSHIHIKO OKADA AND SHINGO TOMITA

***Abstract*—The learning behavior of variable-structure stochastic automata in a three-person zero-sum game is investigated. The game has three variable-structure stochastic automata and a random environment. In the game the players do not possess prior information concerning the payoff matrix, and at the end of every play all the players update their own strategies on the basis of the response from the random environment. Under such situations, if a payoff matrix satisfies some conditions, it can be shown that the learning behavior of the automata converges to the optimal strategies.**

I. Introduction

The learning behavior of variable-structure stochastic automata operating in a random environment has been studied extensively by many authors [1]–[8]. These automata have the capability of learning the desired state by updating their probabilities of actions. Since Chandrasekan and Shen [2] studied the behavior of variable-structure stochastic automata in two-person zero-sum games, various papers on automata games have been published.

Lakshmivarahan and Narendra [6] show that the learning behavior of variable-structure stochastic automata converges to the optimal pure strategies when the game matrix has a saddle point.

However, most of the work in competitive games has been limited to two-person zero-sum games.

Manuscript received April 11, 1983; revised May 1984.
The authors are with the Department of Electronics, Faculty of Engineering, Yamaguchi University, Ube 755, Japan.

0018-9472/84/1100-0924$01.00